ISSN 2543-9901

JOURNAL OF CASTING & MATERIALS ENGINEERING

AGH UNIVERSITY OF SCIENCE AND TECHNOLOGY
FACULTY OF FOUNDRY ENGINEERING

QUARTERLY
Vol. 4 No. 4/2020

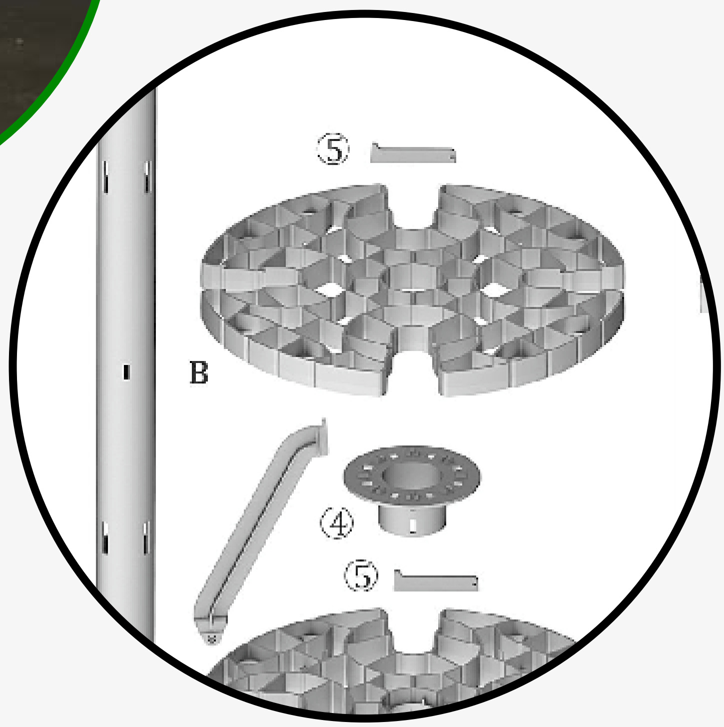

100 YEARS OF AGH UST

JCME

AGH UNIVERSITY OF SCIENCE AND TECHNOLOGY PRESS KRAKOW 2020

The articles published in the Journal of Casting & Materials Engineering have been given a favorable opinion by the rewievers designated by the Editorial Board.

www:
https://journals.agh.edu.pl/jcme/

AGH UNIVERSITY OF SCIENCE AND TECHNOLOGY PRESS KRAKOW 2020

Wydawnictwa AGH (AGH University of Science and Technology Press)
al. A. Mickiewicza 30, 30-059 Kraków
tel. 12 617 32 28, 12 638 40 38
e-mail: redakcja@wydawnictwoagh.pl
http://www.wydawnictwa.agh.edu.pl

Contents

Journal of Casting & Materials Engineering Vol. 4 No. 4 (2020) 53–57
https://doi.org/10.7494/jcme.2020.4.4.53

Structures for Heat Treatment Assembled from Cast Elements

Bogdan Piekarski[a], Andrzej Drotlew[b]

[a]West Pomeranian University of Technology Szczecin, Department of Materials Technology, al. Piastów 17, 70-310 Szczecin, Poland
[b]Przedsiębiorstwo Usług Odlewniczych POLCAST Sp. J., al. Piastów 19, 70-310 Szczecin, Poland
**e-mail: bogdan.piekarski@zut.edu.pl*

Receive 28 May 20202/Accepted: 17 September 2020/ Published online: 4 November 2020
This article is published with open access at AGH University of Science and Technology Press

Abstract

Various types of technological equipment individually designed for operation in pit and elevator heat treatment furnaces are described in this article. A common characteristic of these structures is that they are composed of several or several dozen thin-walled elements of various shapes and sizes, gravity cast in sand moulds from creep-resistant alloys (austenitic Cr-Ni/Ni-Cr cast steel and cast nickel alloys). The design of the castings requires the development of a manufacturing technology that can effectively use the principle of the simultaneous solidification of all components. Properly designed equipment should have minimum weight, maximum strength, and maximum loading capacity combined with adequate durability and reliability. Two designs of the equipment for the heat treatment of steel parts were presented. Both designs, as well as their individual components, were described in detail and illustrated. The main task of the equipment is to form the charge in the furnace and transport this charge both inside and outside the furnace. The first design is the design of an equipment for the heat treatment of large ring-shaped parts. The second design is the design of an equipment, whose structure can be modified using various repeatable components. As a result of these modifications, different variants of the equipment are obtained, allowing for the heat treatment of five different types of the shafts characterized by different shapes and sizes. The study is of an application nature. It is addressed to engineering and technical staff dealing with both the design and operation of heat treatment furnaces.

Keywords:

castings for heat treatment plants, design of castings, grates

1. INTRODUCTION

Heat treatment furnaces are widely used in all industries. One of the basic factors determining their efficiency and reliability is the quality of the technological equipment used to form the charge (the parts subjected to heat treatment) in the furnace working chamber. Another task of the equipment is to transport the charge both in the furnace chamber and in the space of the production hall. It should also be noted that the cost of making or purchasing this equipment contributes significantly to the overall operating cost of the furnace [1–4].

Typical technological equipment for heat treatment is a metal frame on which heat-treated parts are laid. It usually comprises the following main components [4, 5]:

- a grate, which is the base of the frame,
- spacers (other grates can also perform this function) serving as shelves,
- pillar(s) and sleeves, whose length determines the height of the equipment and the distance between the grate and spacers,
- other elements, e.g. hangers, allowing for proper arrangement of heat-treated parts on the frame.

The above mentioned components are primarily assembled by means of detachable connections. Such connections facilitate the exchange of elements when the type of charge is changed and replacement of worn out elements. A loose fit also allows them to undergo a relatively free thermal deformation in the field of their operating temperature [2].

In most cases, better durability and reliability of the equipment can be obtained, when it is made of cast parts and not of wrought semi-finished products. The elements are cast mainly from creep-resistant austenitic Cr/Ni or Ni/Cr cast steel. Occasionally, cast nickel alloys are also used [1–4].

The aim of this study is to present two non-standard designs of technological equipment for the heat treatment of some selected parts. Currently, this equipment is used in the industry, gaining positive opinions from users. The first design is intended for operation in a pit furnace, the second – for operation in an elevator furnace. Both designs are original designs developed by the authors of this study as part of completed projects, and as such are subject to intellectual property protection resulting, among others, from The Act of 4 February 1994 on Copyright and Related Rights, the Act of 30 June 2000 on Industrial Property Law and the Act of 16 April 1993 on Combating Unfair Competition.

2. HEAT TREATMENT EQUIPMENT

Before the Contractor undertakes the heat treatment of the commissioned parts, he must decide whether he can use the already existing technological equipment, or whether the equipment has to be redesigned and custom-made. The choice of the second solution is more likely when the production is of a lot or mass character, or when the parts produced are not typical in respect of the shape, dimensions, weight, and/or properties required after the heat treatment process [1–4].

The equipment discussed in this article was designed for the heat treatment of steel parts, such as:

- rings (Fig. 1a),
- 5 types of shafts (Fig. 1b).

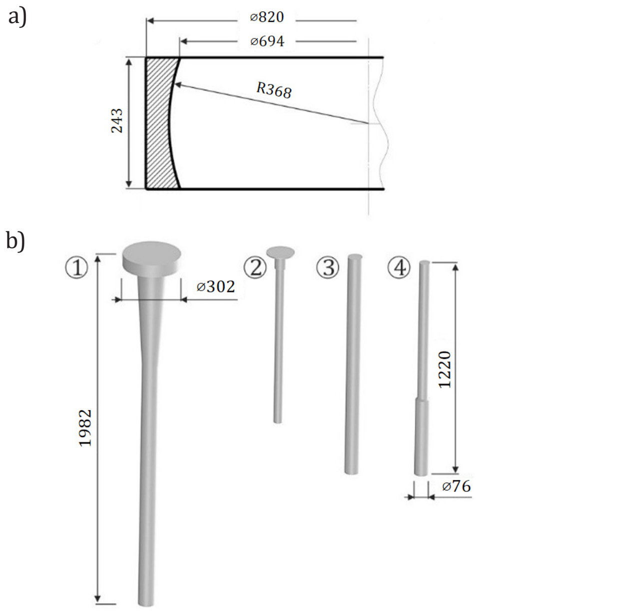

Fig. 1. Heat-treated steel parts: a) ring; b) shafts: 1, 2, 3, 4 – shaft types

2.1. Equipment for the heat treatment of steel rings

To carry out the heat treatment of rings (Fig. 1a), with each ring weighing 230 kg, the technological equipment presented in Figure 2 was constructed in a pit furnace.

The equipment comprises 5 elements (Fig. 3a). Assembled together (Fig. 3), they form a frame on which the heat-treated parts are laid. Elements (Fig. 3a): 1 (pipe/central pillar), 2 (base) and 5 (transport hitch) are permanently connected by welding. Pipe (1 – Fig. 3a) can be made by casting, but a simpler and cheaper solution is to use a seamless steel pipe (e.g. made from 1.4841 steel) with a wall thickness of 8 mm. Elements 3 and 4 do not require a permanent connection – they can be loosely put together. Element 3 is bevelled at corners (see Fig. 3a–b) to place the charge (ring 6 – see Fig. 3b) on the frame using a forklift (Fig. 4).

The designed equipment (Figs. 2 and 3) guarantees a stable position for the heat-treated parts, an adequate flow of atmosphere inside the furnace working chamber, and relatively easy loading and unloading of the charge.

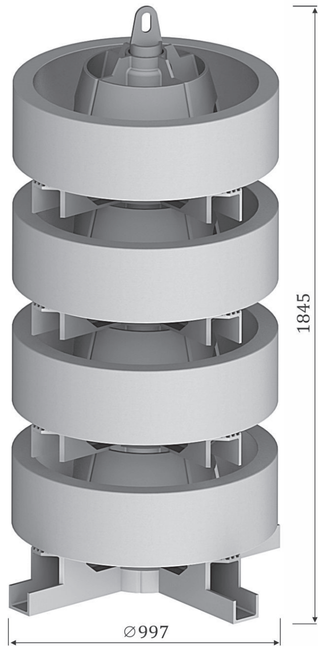

Fig. 2. Technological equipment for the heat treatment of rings (Fig. 1a) loaded with the charge

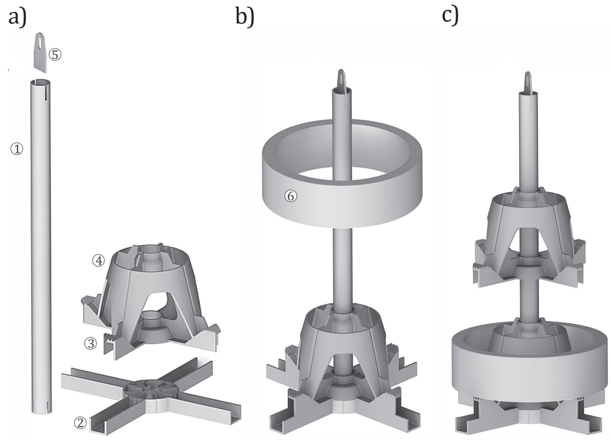

Fig. 3. Parts of the equipment shown in Figure 2 (a) and the method of its assembly and arrangement of the charge – heat-treated rings (b-c). Equipment elements: 1 – pipe/central pillar, 2 – base, 3 – support, 4 – positioning cone, 5 – transport hitch, 6 – heat-treated ring (Fig. 1a)

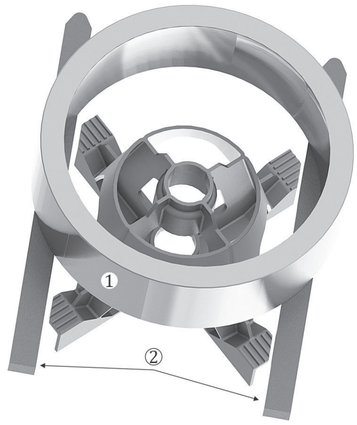

Fig. 4. Ring placed on the frame (Fig. 3) using a forklift: 1 – heat-treated ring, 2 – forklift forks

2.2. Modified equipment for the heat treatment of steel shafts

The equipment designed for operation in the elevator furnace with a working chamber of Ø1000×2100 mm should meet the following conditions:

- allow for the heat treatment of 5 types of shafts (Fig. 1b) each weighing from 20 to 70 kg,
- have a maximum weight of 500 kg together with the charge.

Contrary to the equipment shown in Figure 2, this equipment is designed for operation without the use of a transport hitch.

The charge is placed in the furnace working chamber or pulled out of this chamber using a manipulator which simultaneously grips the equipment with jaws from the bottom and the top.

Three designs of the equipment (designated in further part of the text as **I**, **II**, **III**) were developed, and it was decided to use in each design as many common elements as possible. As a consequence of this decision, the components of the equipment can be divided into the following three groups:

1. Grates (Fig. 5) with the same external dimensions but modified internal design: **A**, **B** and **C**. The type of the heat-treated shaft determines the type of the grate used in the equipment (Fig. 1b). For casting each of the grates, pattern **A** and two types of overlays were used. Their proper imposition on the main pattern allowed the use of cores reproducing:
   - sockets "U" with dimensions smaller in grates **B** and **C** than in grate **A**,
   - sockets with support ribs "D" in grate C (see Fig. 5C).
2. Components of the same shape and dimensions: pipe/central pillar (1), supports (2) and pins (3) (see Fig. 6a – equipment **I**). They are also used in equipment **II** and **III**.
3. Other elements, such as flange (4 – Fig. 7a) and two plugs (5 – Fig. 7a); they are used to position grate **B** in equipment **II** (Fig. 7a) and middle grate **B** in equipment **III** (Fig. 8).

Equipment **I** (Fig. 6). Only shafts of one type are hung in this equipment (1 – Fig. 1b). The equipment consists of the following components (see Fig. 6a):

- grates (**A**, **B**) – 1 piece of each,
- pipe/central pillar (1) – 1 piece,
- supports (2) – 8 pieces,
- pins (3) – 8 pieces.

Grates **A** and **B**. Their central holes have grooves for the positioning of the pillar (1 – Fig. 6) and holes for mounting supports (2) with pins (3).

Supports (2 – Fig. 6a) are used to stiffen the structure of the equipment (see Figs. 6b, 7b-c and 8), position the upper and lower grate and prevent pillar deformation by ensuring the more even distribution of mechanical loads resulting from the presence of the charge. The supports end with a dovetail (a) on one side to enable mounting them in the pillar, and with a yoke (b) on the other side for their assembly on the ribs of the lower and upper grate.

Pillar (1 – Fig. 6a) made from steel or cast steel has three types of slots made by milling:

- the largest slots for fixing supports ending on one side with a dovetail (a),
- smaller (middle) slots for mounting the flange (4) using two plugs (5) (see Fig. 7a). The flange with plugs is used only in equipment **II** and **III**.
- the smallest slots made at the pillar ends. They keep the pillar in position in the lower and upper grate – the pillar is inserted into the grooves made in the central hole of the grate.

Equipment **II** (Fig. 7) is used for the heat treatment of parts 3 and 4 (see Fig. 1b). Compared to equipment **I** (see Figs. 7 and 6), its new elements include flange (4) and two plugs (5) that position grate **B**. Two grates **B** and **C** (Fig. 7a) (see also Fig. 7b-c) are used in the construction of this equipment. The heat-treated shafts (see Fig. 7b-c) "pass" through the openings of grate **B**, while in grate **C** they are resting in appropriately shaped sockets (see also Fig. 5c).

Equipment **III** (Fig. 8) is used for the heat treatment of shaft 2 (Fig. 1b). Shafts are hung on two levels – grates **B**.

In all grates where shafts are hung (equipment **I**, **II** and **III**), the "U" sockets can be additionally milled to make them "deeper" and ensure in this way an equal support for the flanges of the shafts that are heat-treated in a hanging position.

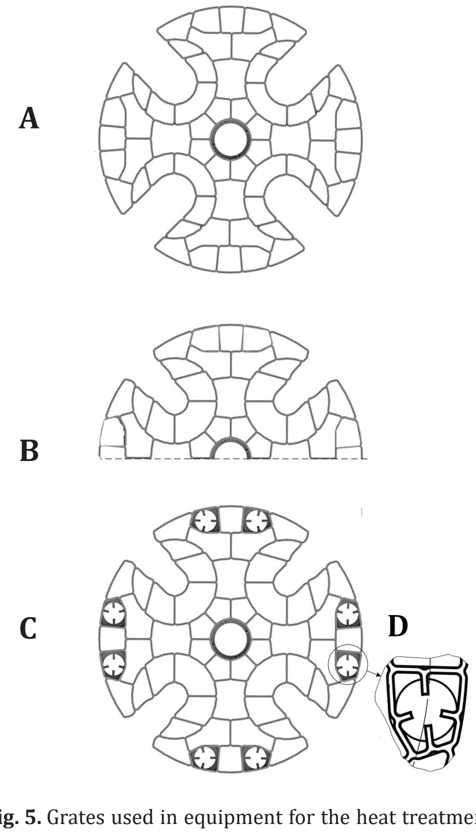

Fig. 5. Grates used in equipment for the heat treatment of shafts: **A**, **B** , **C** – grate types, D – socket with support ribs

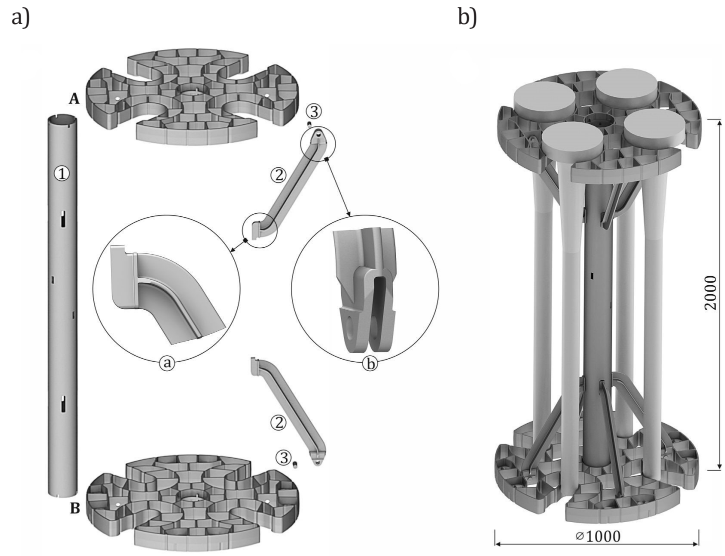

Fig. 6. Equipment **I**. Components of the equipment: A, B – grates, 1 – pipe/central pillar , 2 – support, 3 – pin (a) and equipment with hanging shafts (part 1; see Fig. 1b)

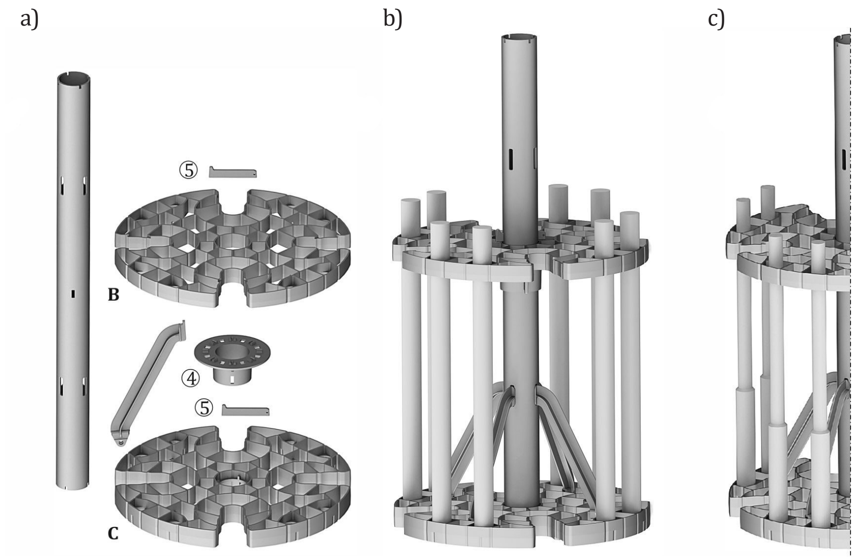

Fig. 7. Equipment **II**. Components of the equipment for the heat treatment of parts 3 and 4 (see Fig. 1b) (a) and positioning of these parts in the equipment: part 3 (b), part 4 (c); 4 – flange, 5 – plugs

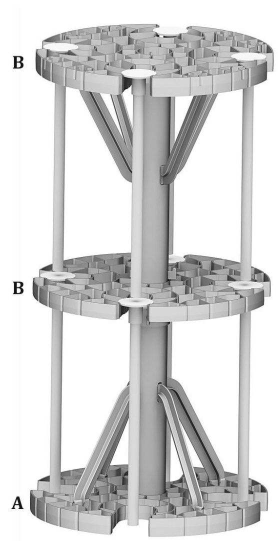

Fig. 8. Equipment **III** for the heat treatment of part 2 (see Fig. 1b)

3. FINAL REMARKS

The design and manufacture of the technological equipment for heat treatment is generally considered to be the most labour-intensive and costly process in the entire preparation of this treatment. Additionally, the design of the equipment has a significant impact on the quality and efficiency of production. It can be assumed that the majority of technical problems which arise during heat treatment are caused by the improper design of the equipment.

Whether or not the technological equipment has been correctly designed and has the required quality mainly depends on the skill, experience, practice and knowledge of the designer, and also on their understanding of the thermal fatigue process which will affect the technological equipment during operation [6–9].

Necessary elements of the designer's knowledge and experience also include the following issues:

- design solutions that can ensure the maximum possible speed of assembly/disassembly of parts of the equipment,
- use of proven technologies for the manufacture and assembly/joining of parts of the equipment,
- use of available means of the mechanization of work, transport and machines to reduce to minimum the time necessary for the preparation of production and performance of heat treatment operations as well as the number of modifications and parts necessary in the equipment,
- knowledge of the available stock of assembled structures and of their versatility which, combined with new adaptation and modernization projects, can significantly facilitate and accelerate all work in the field of implementation of new equipment. In accordance with current trends in the design of this type of equipment, it can also have a modular structure allowing for significant cost reduction and gradual expansion.

Progress in this area of technology is extensively supported by the rapid and continuous development of various methods of designing the technological equipment, with an important contribution being made by IT methods and computer-aided techniques.

REFERENCES

[1] Steinkusch W. (1987). Hitzebeständiger Stahlguss für Wärmebehandlungsanlagen. *Gas Wärme International*, 6, 340–346.

[2] Drotlew A. & Piekarski, B. (2020). Connecting castings for operation under conditions of cyclic temperature changes. *Journal of Castings & Materials Engineering*, 4(1), 16–21.

[3] Davis J.R. (ed.) (1997). *Industrial Applications of Heat-Resistant Materials*. In: Heat Resistant Materials ASM International, 67–85.

[4] Piekarski B. (2012). *Odlewy ze stopów żarowytrzymałych w piecach do obróbki cieplnej.* Szczecin: Wydawnictwo Uczelniane Zachodniopomorskiego Uniwersytetu Technologicznego w Szczecinie.

[5] Folders: Lohmann, Cronite, Pose-Marre, Technoalloy, MANOIR PETRO-CHEM, AFE Technologies, NCK, Polcast.

[6] Piekło J. & Pysz S. (2000). Kształtowanie wytrzymałościowe odlewu palety transportowej stosowanej w piecach tunelowych na podstawie analizy numerycznej pola temperatury i stanu naprężenia. *Biuletyn Instytutu Odlewnictwa*, 1(3), 3–13.

[7] Nandwana D., Bhupendra N.K., Khandelwal N., Bhargava T., Nandwana K. & Jawale G. (2010). *Design, finite element analysis and optimization of HRC trays used in heat treatment process*. Proceedings of the World Congress on Engineering WCE 2010. II, 1149–1154.

[8] Bajwoluk A. & Gutowski P. (2016). Thermal stresses in the wall connections of cast grate structures. *Archives of Foundry Engineering*, 4, 11–16.

[9] Bajwoluk A. & Gutowski P. (2019). Stress and crack propagation in the surface layer of carburized stable austenitic alloys during cooling. *Materials at High Temperatures*, 36(1), 9–18. Doi: 10.1080/09603409.2018.1448528.

Journal of Casting & Materials Engineering Vol. 4 No. 4 (2020) 58–64
https://doi.org/10.7494/jcme.2020.4.4.58

An Evaluation of the Effect of Ultrasonic Degassing on Components Produced by High Pressure Die Casting

Manel da Silva[a]*, Attila Bajusz[b], Thomas Pabel[c], Tose Petkov[c], Xavier Plantà[d]

[a]Eurecat, Centre Tecnològic de Catalunya, Unitat de Materials Metàl•lics i Ceràmics. Avda. Universitat Autonoma 23, Cerdanyola del Vallès, 08290, Spain
[b]Certa Kft., Sátoraljaújhely, 3980, Hungary
[c]Austrian Foundry Research Institute, 8700 Leoben, Austria
[d]Ultrasion, S.L., Cerdanyola del Vallès, 08290, Spain
e-mail: manel.dasilva@eurecat.org

Received: 1 November 2020/Accepted: 23 December 2020/ Published online: 18 January 2021
This article is published with open access at AGH University of Science and Technology Press

Abstract

Ultrasonic treatment is known to be efficient for aluminium melt degassing with the additional benefits of being both economical and environment friendly. This paper describes the effect of ultrasonic degassing on the preparation of an AlSi9Cu3(Fe) alloy for High Pressure Die Casting (HPDC). The degassing efficiency was assessed in terms of the indirect evaluation of the melt, by means of the reduced pressure test and the porosity evaluation of the cast parts. Additionally, the corresponding hydrogen content was estimated with an experimental equation reported in the literature. Ultrasonic degassing shows greater efficiency in terms of hydrogen removal from the melt than conventional N_2 + Ar lance bubbling. Components produced by HPDC without degassing, with ultrasonic degassing and with lance degassing, were analysed by computed tomography and by metallography. The results show that the components produced by HPDC after ultrasonic degassing have a similar porosity level to components degassed with conventional lance bubbling, both showing an important improvement over components produced without degassing treatment. Hardness values were similar for all different treatment conditions and well over the minimum value established for the alloy by the corresponding standard.

Keywords:
aluminium alloy, casting, HPDC, degassing, ultrasonic treatment, hydrogen

1. INTRODUCTION

Hydrogen solubility is relatively high in liquid aluminium and very low in solid aluminium. As a result, the excess hydrogen precipitates during solidification and in most cases gets trapped between solid aluminium grains, forming gas porosity or adding to shrinkage porosity. Porosity is one of the main defects encountered in casting parts and causes poor ductility, low fatigue resistance and reduced strength of the casting. Degassing has become a crucial operation in high quality casting [1].

The dissolved hydrogen present in liquid aluminium mainly comes from atmospheric moisture as water vapour reacts with aluminium to produce alumina and hydrogen. Hydrogen solubility in aluminium is directly correlated to alloy temperature and humidity ratio, therefore lowering the temperature can cause the aluminium to be supersaturated by hydrogen that will tend to naturally degas to the so-called quasi-equilibrium hydrogen level [1–3]. Ultrasonic degassing has the advantage of being able to reach a hydrogen level 50% lower than the quasi-equilibrium concentration [2]. This level of degassing is inevitably followed by natural re-gassing to the quasi-equilibrium level, but this low level of hydrogen can be retained if casting happens shortly after degassing is finished [3].

Ultrasonic degassing of liquid metals has a long history. As early as the 1940s, Esmarch et al. studied the degassing of Al-Mg alloys by vibrations in a crucible and sonic vibrations induced by contactless electromagnetic stirring and [4]. In 1950 Bradfield reported the works of Turner on the degassing of molten aluminium and its alloys by means of the direct introduction of ultrasonic oscillations into the melt at 15 kHz and 26 kHz [5]. Starting from the 1960s, successful laboratory and pilot-scale trials of ultrasonic degassing for foundry and later wrought alloys were performed and summarized in a series of publications by G. Eskin [2, 6]. In these works, the solution to practical issues such as equipment (water-cooled magnetostrictive transducers) and sonotrode materials selection (Nb and Nb-based alloys) were presented and justified; and several practical recommendations were made regarding the degassing schemes and the number of sonotrodes per treated volume [6].

The efficiency of ultrasonic degassing is a function of input ultrasonic power, melt flow, melt temperature, and alloy composition. The fundamental studies on these issues have been published elsewhere [2, 3, 6].

Despite successful industrial trials in the 1960s and 1970s, ultrasonic degassing was not adopted as a mainstream technology due to the arrival of gas-assisted degassing, which steadily replaced little flux degassing treatment, a toxic degassing treatment. In recent years, the intrinsic features of ultrasonic degassing – such as no requirement for gas usage, no toxic or pollutants emissions – led to a reconsideration of this technology since it may answer the current environmental challenges. In addition, the new level of ultrasonic technology has made its application easier.

For this reason, in recent years researchers have been studying the effect that ultrasonic treatment has on metals. However, all these publications are related to laboratory trials, working with a few kilograms of metal [7–9] and very little work has been published regarding results obtained in large melt volumes at industrial scale.

The present paper reports the results of pilot-scale trials of ultrasonic degassing conducted in large volumes (500 kg of aluminium alloy) and the technology's effects on the final cast components produced by High Pressure Die Casting (HPDC), carried out in actual industrial facilities.

2. EXPERIMENTAL PROCEDURE

2.1. Ultrasonic degassing equipment

The experiments were conducted using a prototype specifically designed to treat large volumes of molten aluminium (Fig. 1). The device functioning is described in detail in a previous work, where the results were obtained for a much smaller volume (150 kg) of AlSi7Mg alloy and were compared with rotary degassing [10].

Fig. 1. Image of ultrasonic degassing prototype

The ultrasonic equipment used in the experiments was composed of a 5-kW USGC-5-22 MS ultrasonic generator, a 5-kW MST-5-18 water-cooled magnetostrictive transducer, a titanium booster, all supplied by Reltec (Russia), and a niobium multi-stage sonicator (Fig. 2). Figure 3 shows the assembled ultrasonic degassing equipment used in the experiments.

Fig. 2. Photograph of the stepped sonotrode used in the ultrasonic degassing tests

Fig. 3. Image of ultrasonic equipment used in the trials

2.2. Melt treatment procedure

AlSi9Cu3(Fe) (EN AC-46000) alloy was used for the trials. The treatment was conducted in a holding furnace with a capability of 500 kg, filled up to almost its maximum capacity (over 95%), as is shown in Figure 1. The alloy was previously molten in a tilting tower furnace and was transferred to the holding furnace with a standard transport ladle with a capacity of 200 kg, without performing any treatment or skimming process to the melt. The degassing treatment was conducted at a metal temperature of 690 ±10°C.

A stepped sonotrode as shown in Figure 2 was used to treat the molten metal during 15 min. During the ultrasonic treatment (US) the sonotrode was moved with the rotary crown of the prototype inducing circular movements at approximately 2/3 of the crucible diameter at a rotational speed of about 1 rpm [10]. Research conducted previously suggests that in order to treat large volumes the ultrasonic treatment must necessarily be long with a moving ultrasonic stream within the melt surface [3]. Ultrasounds with power between 4.0 and 4.5 kW in the range of 17–18 kHz were applied to the molten metal with an approximated vibration amplitude of 25 µm. Alternatively, a 15 min degassing treatment with a porous graphite lance bubbling an N_2 + Ar mixture, was introduced to the same amount of metal, with the same temperature and composition.

Indirect measurements of the hydrogen content with Reduced Pressure Test (RPT) (MK, Germany) were performed before and after the degassing treatment in the holding furnace. The values of the resulting Density Index (DI) were calculated form the extracted samples. The corresponding hydrogen content was calculated by applying an empirical equation reported in the literature for AlSi9Cu3(Fe) alloy [3].

2.3. Component casting and evaluation

The cast components were produced using a HPDC Unit (Weingarten 250 Tn) with a 50 mm plunger diameter, 3 m/s of injection speed and 180–220 bar of compacting pressure. For the casting production, the melt was transferred from the holding furnace to the shot sleeve with a rotary transport ladle. A standard production die of an actual industrial component was used to cast the specimens. Die lubrication and extraction of the part were done manually by an operator.

The HPDC components were produced in two different batches. From the 1st batch components were produced in three different ways; without treatment (W), with US treatment (0 holding time) and US1.5 (1.5 hours holding time after US treatment). From the 2nd batch, components were produced with a 15 min lance degassing treatment. The L (0 holding time) and L1 (after 1 hour holding time) components belong to this 2nd batch. One piece produced in each of these degassing conditions were analysed (treatment + waiting time).

The porosity of the selected parts (Fig. 4a), was analysed by computed tomography v|tome|x (with area detector DXR-250RT, magnification of 6.23, acceleration voltage of 180 kV, current of 200 µa, filter of 2 mm Al, exposure time of 333 ms and voxel size of 342.885 × 10^{-6} mm^3). This setup allows to detect pores with a minimum size of 140 µm.

The same parts were subsequently sectioned in order to measure their chemical composition, microstructure and hardness. Figure 4b shows the regions where the different specimens were extracted from. The chemical composition of these sections were analysed by optical emission spectrometry with a Spectrolab analyser from Spectro. An Olympus optical microscope was used for the microstructural analysis. The porosity of the polished specimens was quantified with Analysis software, at a magnification of 100×, what implies the screening of a total area of 1.63 mm^2 per image. A Zeiss Gimini Field Emission Scanning Electron Microscope (FE-SEM) was used to determine the different intermetallic phases present in the alloys with the aid of the Energy Dispersive Spectroscopy (EDS) detector.

The hardness of the components was determined with a Brinell HB10 (62.5 Kpf/2.5). A total of 6 indentations were performed in each component.

a)

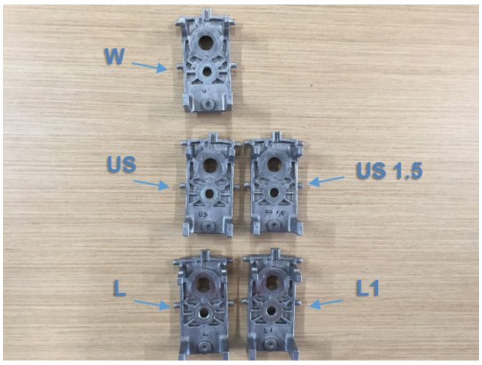

b)

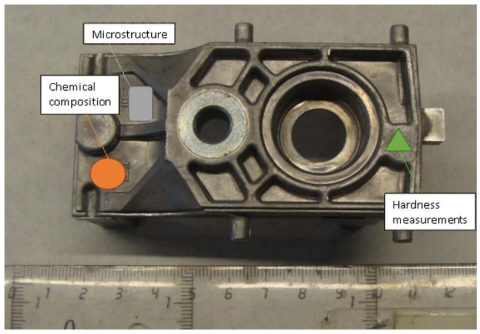

Fig. 4. Images of: a) the components selected for characterization; b) the location where the different characterization techniques were applied

3. RESULTS AND DISCUSSION

3.1. Melt quality

The results of the RPT measures conducted in the molten aluminium before and after the degassing treatments are presented in Figure 5. The graph shows the decrement of the DI after the corresponding degassing treatment. The DI values are much smaller after the US treatment, which shows that this treatment is much more effective than the lance degassing using an N_2+ Ar mixture.

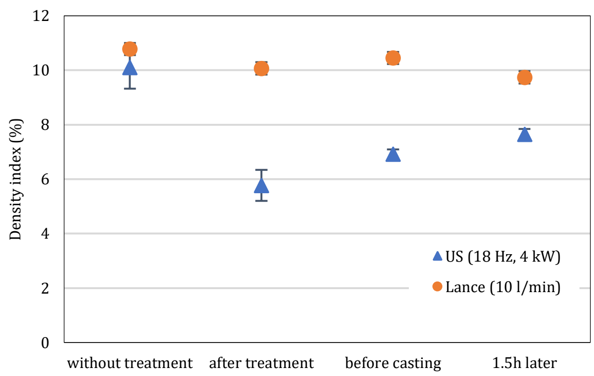

Fig. 5. Density index values obtained after ultrasonic treatment (US) and after lance degassing treatment (Lance)

The hydrogen content present in the melt can be estimated from Equation (1) [3]:

$$[H] = (DI + 0.0204)/0.5066 \quad (1)$$

The measured DI values and the corresponding hydrogen contents calculated with Equation (1) are presented in Table 1.

Table 1
Density Index values obtained in the melt analysis and their corresponding estimated hydrogen concentration

Treatment type	Ultrasounds		Lance bubbling	
Stage	**DI (%)**	**H (cm^3/100 g)**	**DI (%)**	**H (cm^3/100 g)**
Before treat	10.10	0.240	10.78	0.253
15 min after	5.77	0.154	10.07	0.239
Before cast	6.92	0.177	10.45	0.247
1.5 h later	7.65	0.191	9.74	0.232

These measurements show that, while ultrasonic degassing reduces the original DI values from about 11 to 6, the lance decreases the DI only to about 10, in the AlSi9Cu3(Fe) alloy. On one hand, these high DI values obtained for the lance degassing suggest that the degassing efficiency of this treatment is not as high as modern rotary degassing [11]. On the other hand, these values confirm that ultrasound is a more effective degassing method to remove H2 than the standard lance degassing treatment currently used by the foundry for the AlSi9Cu3(Fe) alloy. 36% lower hydrogen level was observed 15 minutes after the US degassing treatment than for lance degassing and this reduction remained still at 28% just before casting started

The values of DI and their corresponding equivalent hydrogen level slightly increases with the subsequent holding time in the case of the ultrasonic treatment. This effect can be attributed to the natural re-gassing taking place in the alloy, as it was already reported for AlSi9Cu3(Fe) alloy for smaller melt volumes. This phenomenon takes place after effective degassing treatment, i.e. those which reduce the hydrogen concentration below the corresponding quasi-equilibrium level of the melt [3].

On the other hand, the efficiency of lance degassing in such a large volume is quite small. The initial degassing effect is very small, decreasing the DI value from 11 to 10, and with the holding time, the DI values remain at the same level or even slightly decrease, suggesting that a natural degassing may still been taking place. The results suggest that lance bubbling in such large volumes is not an efficient means for aluminium degassing.

3.2. X-ray tomography analysis

The 3D reconstruction of the pore distribution obtained by the X-ray tomography is presented in Figure 6 for two of the die-casted components analysed, without treatment (W) (Fig. 6a) and treated with US (US) (Fig. 6b). The defects are concentrated in both cases in the lower part of the component, mainly in the junction between the main body and the two lower arms, as it can be observed in the images.

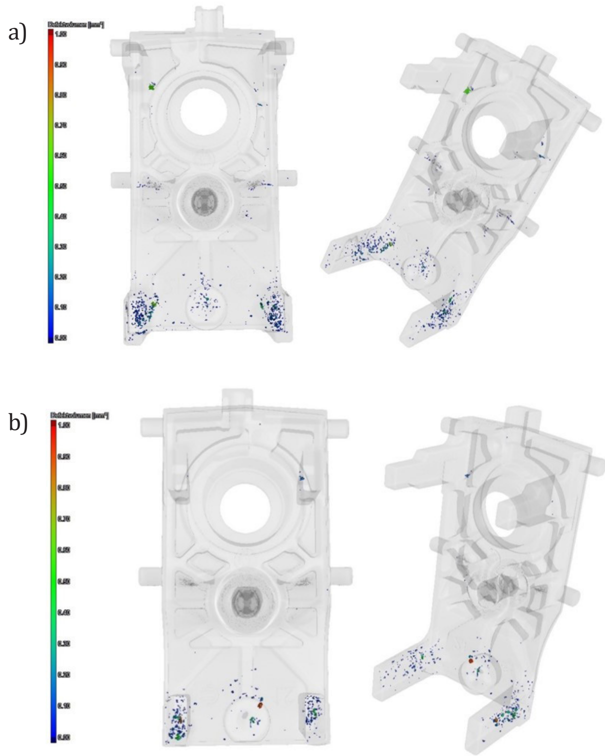

Fig. 6. 3D reconstruction of the porosity from the tomography images of: a) a part without degassing treatment; b) a part with ultrasonic degassing treatment

A comparison of the pores observed in the inspected components by X-ray tomography is presented in the form of a histogram in Figure 7. It can be observed that both degassing treatments considerably reduce the number of pores, especially of small pores, even though no difference can be observed in the porosity distribution of the parts produced by HPDC regarding the degassing treatment conducted, presumably due to the high porosity intrinsically related to this casting process [12].

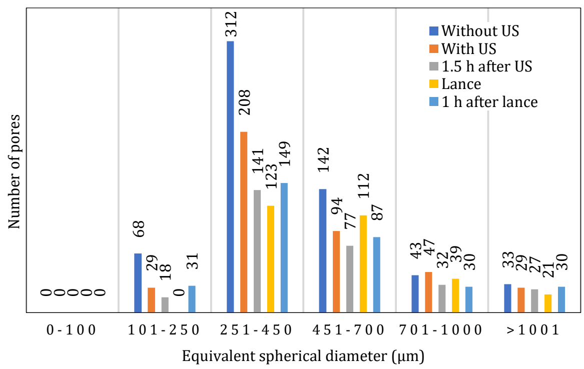

Fig. 7. Pore distribution for the different components measured by computed tomography

Therefore, the difference in degassing efficiency perceived from the DI values measured in the melt after the degassing treatment is diluted once the HPDC process is applied, obtaining components with a similar degree of porosity level.

3.3. Chemical composition and microstructure

The chemical composition of the two batches used to produce the components is presented in Table 2. The composition values of the batches are very similar and is in the composition range defined in the UNE-EN 1706-2011 standard for alloy EN AC-AlSi9Cu3(Fe).

Table 2
Chemical composition of the material used to produce the HPDC components

Batch	%Si	%Fe	%Cu	%Mn	%Mg	%Zn	%Pb
W-US	8.75	0.75	2.46	0.21	0.32	1.02	0.08
L	8.89	0.76	2.53	0.21	0.32	1.03	0.08
EN AC-AlSi9Cu3(Fe) UNE-EN 1706-2011	8–11	< 1.3	2–4	< 0.55	0.05 –0.55	< 1.2	< 0.35

The microstructure of the cross sections of the castings produced after any of the degassing treatments is typical for this type of alloy and consists of a primary Al-solid solution and (Al + Si)-eutectic. Figure 8 shows the microstructure of samples produced without treatment (W), with lance bubbling (L and L1) and with ultrasonic degassing (US and US1.5). Table 3 shows the results obtained from the porosity quantification performed on the polished specimens. It can be observed that the porosity level of the 5 specimens fell in the same range (between 0.1 and 0.6%), corroborating the results obtained by X-ray tomography, that porosities in both set of components are in the same level.

In addition to the main structural phases, isolated Fe-containing particles in the form of polygonal particles and of a needle shape were observed in the FE-SEM analysis (Fig. 9). These intermetallic phases are formed due to the presence of Fe in the alloy and, by contrast, these can be distinguished from Si particles. From the EDS analysis performed in the FE-SEM and from the phases reported in the literature for Al–Si–Cu alloys with similar composition [13], it is deduced that the Fe-containing intermetallic compounds present in the alloy are (Fe,Mn)3Si2Al15, polygonal phases (Spectrum 1), and FeSiAl5, elongated phases (Spectrum 4). It can be observed that Spectrum 4 has a high amount of Cu as well. As the elongated FeSiAl5 phases are quite narrow and are commonly surrounded by rich Cu phases, such as CuAl2, the area covered by the X-ray analysis contains also part of this surrounding material. In the microstructure there is no indication of over-modifications such as polygonal Al2Si2Sr intermetallic phases or coarsened Si-eutectic. Non-metallic inclusions, i.e. oxides and oxide films, were detected.

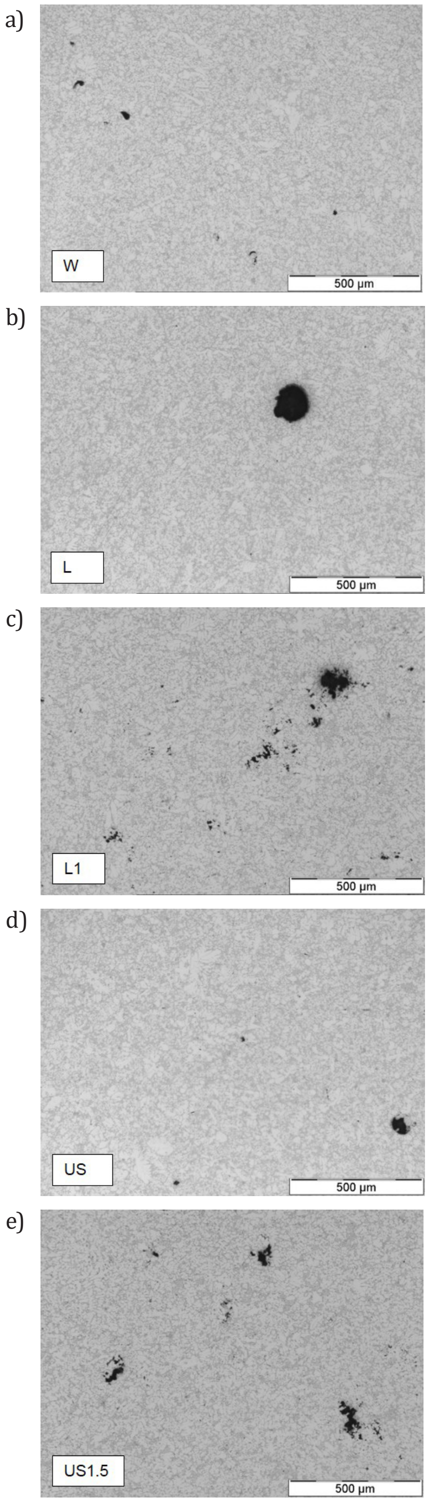

Fig. 8. Microstructure of the components: a) produced without heat treatment (W), b) produced immediately after applying the lance degassing treatment (L), c) produced after approximately 1 hour of production time (L1), d) produced after ultrasonic degassing treatment (US) and e) produced about 1.5 hours after the treatment (US1.5)

Table 3
Porosity values in the different HPDC components measured by quantitative metallography

Component ref.	W	L	L1	US	US1.5
Porosity (%)	0.13	0.1	0.58	0.23	0.28

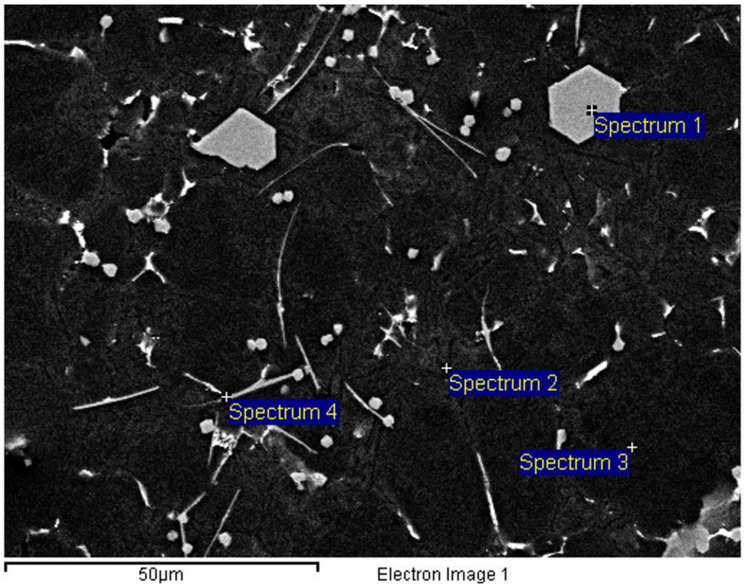

Processing option : All elements analysed (Normalised)

Spectrum	Al	Si	Cr	Mn	Fe	Ni	Cu	Zn	Total
Spectrum 1	59.12	9.59	1.68	7.91	19.70		2.00		100.00
Spectrum 2	83.77	12.56					2.28	1.39	100.00
Spectrum 3	98.21						0.89	0.90	100.00
Spectrum 4	65.33	10.19		0.78	6.16	0.64	15.07	1.83	100.00

Fig. 9. FE-SEM image with EDS analysis of the different phases observed in the AlSi9Cu3 alloy

3.4. Mechanical properties

The obtained values from the hardness measurements are shown in Table 4. The average hardness values of all the castings are in the range of 93–95 HB, which is well above the minimum hardness of 80 HB 5/250 required by UNE-EN 1706:2011 for AlSi9Cu3(Fe) alloy. No significant difference in hardness can be observed between the components produced with different degassing treatments.

Grain refining effect is commonly associated with ultrasonic treatment [14, 15], however, no evidence of it was observed with this experimental set-up. Even, if it is quite controversial to directly apply the Hall–Petch equation in Al-Si casting alloys, various authors have reported a clear relation between grain size, yield and tensile strength and hardness. Values of hardness and material strength increase with grain refinement [16–18].

Table 4
Brinell HB10 hardness obtained for the HPDC parts

Indentation	W	L	L1	US	US1.5
1	93	97	98	89	89
2	91	89	90	86	87
3	97	101	97	97	97
4	90	94	91	94	93
5	94	90	101	97	92
6	96	99	95	95	97
Average	94±3	95±6	95±5	93±5	93±5
EN AC-AlSi9Cu3(Fe) UNE-EN 1706-2011	min 80	–	–	–	–

As explained before, hardness values are at the same level for both degassing treatments, which indicates that grain size is in a similar level for both materials. Grain refining may take place when the ultrasonic treatment is conducted in a melt with a reduced superheat and shortly before the solidification takes place [14, 15]. In the present work, the metal was treated at a temperature of more than 100°C over the liquidus of the alloy and between the ultrasonic treatment and the alloy solidification at least several minutes passed and a transfer movement occurred and these processing conditions may prevent grain refining [19].

4. CONCLUSIONS

From the results obtained, the following conclusions can be inferred from the present study:

- The ultrasonic technology at a prototype level studied in this article shows a better degassing efficiency, lowering the hydrogen content in a large industrial melt volume of 500 kg of AlSi9Cu3(Fe) by 28% to 36% when compared to the work of a porous lance, a commercially available degassing technology.
- The better degassing efficiency of the US treatment is mitigated by the HPDC process, obtaining castings with a similar porosity level to lance degassing.
- The obtained hardness values are well above the minimum values established in the standard for the alloy and are similar for the different treatment conditions analysed, suggesting that the present experimental set-up does not promote a grain refining effect on the final component.

Acknowledgements

The authors would like to acknowledge the financial support provided by the European Union's Seventh Framework Program managed by REA – Research Executive Agency (FP7/2007-2013) under Grant Agreement number 286344 (www.doshormat.eu). The authors gratefully acknowledge all of the help provided by the members of the consortium.

REFERENCES

[1] Campbell J. (2003). *Castings*, 2nd Ed. Oxford: Butterworth--Heinemann.

[2] Eskin G. & Eskin D. (2014). *Ultrasonic Treatment of Light Alloy Melts*, 2nd Ed. Boca Raton: CRC Press.

[3] Eskin D., Alba-Baena N., Pabel T. & da Silva M. (2015). Ultrasonic degassing of aluminium alloys: basic studies and practical implementation. *Materials Science and Technolgy*, 31(1), 79–84. Doi: https://doi.org/10.1179/1743284714Y.0000000587.

[4] Esmarch W., Rommel T. & Benther K. (1940). *Werkstoff-Sonderheft*. Berlin: W.V. Siemens Werke, 78–87.

[5] Bradfield G. (1950). Summarized Proceedings of Symposium on Applications of Ultrasonics. *Proceedings of the Physical Society B*, 305–321. Doi: https://doi.org/10.1088/0370-1301/63/5/301.

[6] Eskin G. (1965). Ul'trazvukovaya obrabotka rasplavlennogo alyuminiya [*Ultrasonic Treatment of Molten Aluminum*]. Moskva: Metallurgija. [Эскин Г. (1965). *Ультразвуковая обработка расплавленного алюминия*. Москва: Металлургия].

[7] Xu H., Meek T.T. & Han Q. (2008). Effect of ultrasonic vibration on degassing of aluminium alloy. *Materials Science and Engineering A*, 473(1–2), 96–104. Doi: https://doi.org/10.1016/j.msea.2007.04.040.

[8] Puga H., Barbosa J., Tuan N.Q. & Silva G. (2004). Effect of ultrasonic degassing on performance of Al-based components. *Transactions of Nonferrous Metals Society of China*, 24 (11), 3459–3464. Doi: https://doi.org/10.1016/S1003-6326(14)63489-0.

[9] Galarraga H., Garcia de Cortazar M., Arregi E., Iparraguirre J.A. & Oncala J.L. (2018). Improved ultrasonic degassing of AlSi10Mg alloy and its performance evaluation with reducer pressure test (RPT) method. *The 73rd World Foundry Congress: September 23–27. Krakow*. World Foundry Association Ltd., 337–338.

[10] da Silva M., Rebolledo L., Pabel T., Petkov T., Planta X., Tort J. & Eskin D. (2015). Evaluation of effect of ultrasonic degassing on components produced by low pressure die casting. *International Journal of Cast Metals Research*, 28 (4), 193–200. Doi: https://doi.org/10.1179/1743133614Y.0000000141.

[11] Ignaszak Z. & Hajkowski J. (2015). Contribution to the Identification of Porosity Type in AlSiCu High-Pressure-Die-Castings by Experimental and Virtual Way. *Archives of Foundry Engineering*, 15(1), 143–151.

[12] Niklas A., Orden S., Bakedano A., da Silva M., Nogués E. & Fernández-Calvo A.I. (2016). Effect of solution heat treatment on gas porosity and mechanical properties in a die cast step test part manufactured with a new AlSi10MnMg(Fe) secondary alloy. *Materials Science and Engineering A*, 667(14), 376–382. Doi: https://doi.org/10.1016/j.msea.2016.05.024.

[13] Mondolfo L.F. (1976). *Aluminum Alloys. Structure & Properties*. London: Butterworth & Co., 759–805.

[14] Powell M., Manchiraju K. & Han Q. (2016). Ultrasonic grain refining of continuous cast aluminium: microstructure and properties. *TMS Conference Light Metals: February 14–18. Nashvile*, 737–740. Doi: https://doi.org/10.1007/978-3-319--48251-4_124.

[15] Haghayeghi R., Ezzatneshan E. & Bahai H. (2015). Grain refinement of AA5754 aluminium alloy by ultrasonic cavitation: experimental study and numerical simulation. *Metals and Materials International,* 21, 109–117. Doi: https://doi.org/10.1007/s12540-014-6015-5.

[16] Ghassemali E., Riestra M., Bogdanoff T., Bharath S. Kumar & Seifaddine S. (2017). Hall–Petch equation in a hypoetutectic Al-Si cast alloy: grain size vs. secondary dendrite arm spacing. *Procedia Engineering*, 207, 19–24. Doi: https://doi.org/10.1016/j.proeng.2017.10.731.

[17] Basavakumar K.G., Mukunda P.G., Chakraborty M. (2008). Influence of grain refinement and modification on microstructure and mechanical properties of Al-7Si and Al-7Si-2.5Cu cast alloys. *Materials Characterization*, 283–289. Doi: https://doi.org/10.1016/j.matchar.2007.01.011.

[18] Tiryakioglu M., Campbell J., Staley J. (2000). Hardness-Strength Relationships in Cast Al-Si-Mg Alloys. *Materials Science Forum*, 331–337, 295–300. Doi: https://doi.org/10.4028/www.scientific.net/MSF.331-337.295.

[19] Piatkowski J., Przeliorz R., Gontarczyk A. (2016). The study of phase transformations of AlSi9Cu3 alloy by DSC method, *Archives of Foundry Engineering*, 16 (4), 109–112. Doi: https://doi.org/10.1515/afe-2016-0093.